WiLiTV: Reducing Live Satellite TV Costs Using Wireless Relays

Rajeev Kumar, *Student Member, IEEE*, Robert Margolies, *Member, IEEE*, Rittwik Jana, *Member, IEEE*, Yong Liu, *Fellow, IEEE*, and Shivendra S. Panwar, *Fellow, IEEE*

***Abstract*— The bandwidth required for TV content distribution is rapidly increasing due to the evolution of high definition TV (HDTV) and ultra HDTV. Service providers are constantly trying to differentiate themselves by innovating new ways of distributing content more efficiently with lower cost and higher penetration. We propose a cost-efficient wireless architecture [wireless live TV (WiLiTV)], consisting of a mix of wireless access technologies [satellite, Wi-Fi, and LTE/5G millimeter wave (mmWave) overlay links], for delivering live TV services. In the proposed architecture, live TV content is injected into the network at selected locations, consisting of some homes and/or cellular base stations, using satellite antennas. The content is then further distributed to other homes using a house-to-house Wi-Fi network or an LTE/5G mmWave overlay. We construct an optimal content distribution network with the minimum number of satellite injection points, while preserving the highest quality of experience, for different neighborhood densities. We evaluate the framework using time-varying demand patterns and a diverse set of home location data provided from an operational content distribution network. Our study demonstrates that this architecture reduces the overall cost by 60% compared with the traditional architecture. We have also shown that the WiLiTV is robust in its support for several TV formats.**

***Index Terms*— Live TV distribution, QoE, low cost architecture, 5G, mmWave, IPTV, satellite TV, WiFi, LTE.**

I. Introduction

With the evolution of HDTV, 4K content, and the prevalence of hundreds of channels, the need for bandwidth is ever increasing [1]. Even with advanced video compression techniques, each Standard, High Definition, and Ultra-High Definition TV (SDTV, HDTV, and UHDTV) channel requires 2, 9, and 15.6 Mbps, respectively. Today, the vast majority of houses receive TV content via cable to the home (cable TV), over an IP network (Internet Protocol TV), or through a satellite (satellite TV) [2]. As illustrated in Fig. 1(a), the Internet Protocol TV (IPTV) streams live TV content from a few regional hub offices to set-top boxes over either a dedicated private network or over-the-top via the core IP network [3]. To satisfy Quality of Service (QoS) requirements, IPTV must be provisioned with a sufficiently high bandwidth in the core and distribution networks [4]. According to FCC's 2014 data, downlink broadband speed to houses in the US varies from 2.4 Mbps to 15.9 Mbps with a median speed of 6.7 Mbps [5] that cannot satisfy the bandwidth requirements of HDTV/UHDTV. Thus, the current infrastructure will soon be stressed with this escalating demand.

One solution to the growing demand is to deploy more fiber to scale up the capacity of both backbone and distribution networks; however, this will result in greater infrastructure cost [6] and higher energy consumption [7]. Deployment of more fiber is an expensive solution and on average costs $22,000/mile [8]. WiFi technology, on the other hand, is a cost-effective solution used to provide access over the last mile by many vendors and service providers [9], [10]. Further, the overall infrastructure cost can be reduced by pushing live TV traffic to end-users or the edge of the network [11]. Similarly, 5G mmWave can decrease backhaul cost significantly by providing multi-gigabit connectivity to households from the nearest TV injection points [12]. Satellite TV providers avoid the wired infrastructure cost by broadcasting live TV content to *every* home equipped with a dish antenna. However, satellite providers incur a high initial cost to install a dish antenna at each new customer home. In New York, for example, installing a single satellite dish costs approximately $1,000 [13].

To distribute TV content at lower cost with higher penetration, we propose a low-cost, Wireless Live TV (WiLiTV) architecture that leverages a range of access technologies (Satellite, WiFi, and LTE/5G mmWave) to provide high quality live TV services. As shown in Fig. 1(b), the WiLiTV architecture strategically equips a few houses and/or LTE/5G mmWave Base Stations (BSs) with satellite antennas and relays TV content to other homes using WiFi and/or cellular networks. Our proposed architecture offloads TV content from the traditional core IP network or a dedicated wired IPTV infrastructure to long-haul satellite links and local high speed wireless links among houses, with the potential of leveraging recent advances in wireless technologies, such as Massive MIMO and mmWave. With this novel architecture, our design goal is to satisfy the live TV demands of all houses at the lowest possible infrastructure cost. To quantify the savings from such an architecture, we need to solve two sub-problems:

- *Source Provisioning:* which houses are chosen to install satellite antennas and download all live TV channels?

Manuscript received July 1, 2017; revised November 14, 2017; accepted January 20, 2018. Date of publication February 8, 2018; date of current version March 29, 2018. This work was supported in part by AT&T Labs, in part by the NYU Wireless, and in part by the New York State Center for Advanced Technology in Telecommunications. *(Corresponding author: Rajeev Kumar.)*

R. Kumar, Y. Liu, and S. Panwar are with the Department of Electrical and Computer Engineering, Tandon School of Engineering, New York University, Brooklyn, NY 11210 USA (e-mail: rajeevkr@nyu.edu; yongliu@nyu.edu; panwar@nyu.edu).

R. Margolies was with AT&T Labs, Bedminster, NJ 07921 USA. He is now with Google, New York, NY 10011 USA (e-mail: margolies.rob@gmail.com).

R. Jana is with AT&T Labs, Bedminster, NJ 07921 USA (e-mail: rjana@research.att.com).

Color versions of one or more of the figures in this paper are available online at http://ieeexplore.ieee.org.

Digital Object Identifier 10.1109/JSAC.2018.2804040

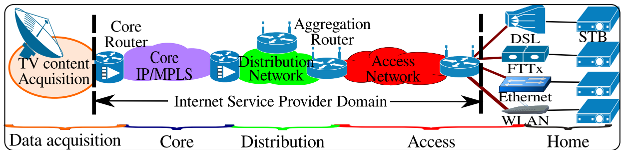

(a) Traditional IPTV architecture

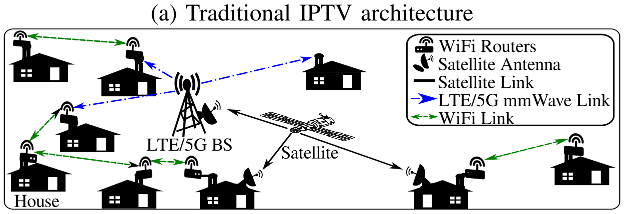

(b) *Our proposed WiLiTV architecture:*- content is first delivered to a community through a few selected houses and LTE/5G BSs with satellite antennas, and is then distributed to other houses using WiFi and LTE/5G mmWave.

Fig. 1. Comparison of IPTV and our proposed WiLiTV architectures.

- *Relay Routing:* how should the live TV channels requested by each house be relayed from the sources?

These two sub-problems are tightly coupled: source provisioning determines the potential sources that a household can download content from; and if some households cannot find a relay routing solution to get their desired channels, new sources have to be added to the distribution network. There is a fundamental trade-off between the complexity of relay routing and the cost saving in source provisioning. The current satellite TV providers, such as Dish Network [14], are at one end of the trade-off spectrum, where each household installs a satellite antenna and no relay routing is needed at all. At the other end, one can minimize the number of satellite antennas to be installed by maximally utilizing any possible wireless relay routing among households to satisfy their live TV demands. However, multihop wireless relay suffers from bandwidth constraints, longer delay, and lower reliability as the number of hops increase. Thus, any practical solution has to find the sweet point and strike the right balance between complexity and cost-saving such that the QoE requirements can be satisfied. To systematically evaluate the impact of various relay routing factors on cost saving, we formulate a series of joint provisioning-routing optimization problems to find the lowest costs under different routing constraints, including relay hop count limit, splittable or non-splittable flows, LTE/5G mmWave availability, and dynamic or static solutions. The optimization models developed are used to numerically investigate the routing complexity and cost saving tradeoff through case studies with real household topology and user demand data. The key contributions of this paper are:

1) We propose the WiLiTV architecture to provide high quality live TV services to users via a mix of wireless access technologies (i.e., satellites, WiFi relayed communication, and LTE/5G mmWave overlay network).
2) We formulate a series of novel joint optimization problems to systematically evaluate the trade-off between the cost saving in satellite antenna provisioning and the complexity in relay routing, considering various practical provisioning and routing constraints.
3) The formulated optimization problems are solved using binary integer programming, or mixed-integer programming for small and medium networks. For large networks, we develop a set-cover based greedy heuristic algorithms to obtain close-to-optimal solutions.
4) We evaluate the proposed WiLiTV architecture using real household topology and user demand data from a major live TV service provider for urban, suburban and rural scenarios. Our results demonstrate that WiLiTV requires 85% to 90% fewer satellite injection points, compared to the traditional satellite TV architecture. Most of the cost savings can be achieved with simple and practical relay routing solutions. Further, WiLiTV architecture reduces the total cost of live TV service provisioning by 60% of the cost of the traditional satellite TV architecture.
5) We evaluate the tolerance of the obtained optimal relay topology to WiFi link degradation using linear programming. Our results show that the optimal topology can tolerate up to 17%, 23%, and 34% WiFi link degradation in the rural, suburban, and urban scenarios, respectively.
6) Finally, we evaluated WiLiTV architecture for different TV formats (SDTV, HDTV, and UHDTV). Our results show that WiLiTV architecture is robust in its support of different TV formats.

This paper is organized as follows. In Section II we discuss the related work. The system model and assumptions made are described in Section III. The optimization problem formulations are presented in Section IV. Section V and Section VI contain the associated solution techniques and the numerical results, respectively. Section VIII concludes the paper.

II. Related Work

Satellite broadcasting systems [15] has been evolving continuously since their first commercial deployment in the 1970s. The advancement in channel coding and modulation, digital video compression, and the maturity of Ka-band has attracted research attention towards interactive satellite TV services and TV-centric triple play services to homes using Digital Video Broadcasting-Satellite-Second Generation (DVB-S2) [16], [17]. Further, these advancements have also opened the possibility of commercial UHDTV broadcast services [18]. Morosi *et al.* [19] proposed hybrid satellite/terrestrial cooperative relaying strategies for digital video broadcasting-satellite services to a handheld device based communication system to enhance reliability and connectivity in telecommunication networks. They have shown that the Bit Error Rate (BER) can be improved significantly using hybrid satellite/terrestrial cooperative relaying strategies. Further, cooperative terrestrial satellite communication can be helpful for improving outage probability and coverage extension [20], [21]. In this work, we focus on the advancement of satellite communications to deliver HD/UHD TV content to households at a lower cost while maintaining high QoE. Our proposed architecture exploits recent advancements in satellite and terrestrial wireless systems to enhance connectivity and QoE.

Another TV content distribution architecture is IPTV (see Fig. 1(a)) that can be divided into five main parts, (i) a data acquisition network, (ii) a core backbone network containing super hub offices, (iii) a regional distribution network containing video hub offices, (iv) an access network containing DSLAMs, and (v) the customer home network containing residential gateways and set-top-boxes [22]. To decrease bandwidth requirements in the core backbone network and for fast TV channel switching, multicast channels and groups are typically used [23]. However, building and pruning multicast groups put an extra burden on the network. It is also costly to maintain multicast groups for less popular TV channels [24].

Peer-to-peer (P2P) is another technology that has been investigated for distributing live TV. In P2P IPTV each user is also a potential server, multicasting received content to other users [22], [25]. However, there are challenges associated with P2P to accommodate fast TV channel switching and TV channel recovery, especially when streaming peers leave the system abruptly. This can result in an interruption while viewing live TV and eventually a poor QoE. In our proposed WiLiTV architecture, we push TV content close to end users, which reduces the delays associated with channel switching. Additionally, unicast flows for requested TV channels makes the WiLiTV architecture suitable for less popular channels.

In our previous work [26], we showed that around 84%-88% of the satellite antenna cost can be saved using WiLiTV architecture using all-or-nothing flows (a node can receive traffic from only one source/relay node). In this work, we further explore different routing possibilities to minimize the total operational cost of WiLiTV. Further, we consider 5G mmWave backhaul to provide high-quality TV services. We also evaluate the tolerance limit of optimal WiLiTV with WiFi link degradation. This work illustrates the feasibility of local wireless networks such as WiFi, LTE, and 5G mmWave for provisioning of high-quality services, evaluates the proposed WiLiTV architecture with additional routing options to minimize cost while satisfying required QoE requirements, and presents the maximum degradation tolerance limit of wireless links without compromising QoE.

III. System Model and Assumptions

As illustrated in Fig. 1(b), our wireless distribution network for live TV consists of three types of nodes:

1) A subset of houses equipped with satellite antennas act as the injection points for live TV content. They also have WiFi APs for relaying content to WiFi-only houses.
2) LTE/5G mmWave BSs equipped with satellite antennas act as additional live TV injection points, and can deliver content to LTE/5G mmWave-enabled houses over lightly loaded LTE bands or 5G mmWave bands.
3) Houses which do not have satellite antennas, but are equipped with WiFi APs and/or LTE/5G mmWave receivers, can receive TV content from houses having satellite antennas over the WiFi network and/or LTE/5G mmWave overlay. These houses can also relay traffic to other houses using WiFi.

As a result, a household can receive TV content by the following methods: (i) directly from a satellite antenna at their own home, (ii) through WiFi relay from a satellite equipped home, (iii) through a satellite equipped LTE/5G mmWave BS, and (iv) through both a satellite equipped LTE/5G mmWave BS followed by WiFi relays. Fig. 1(b) illustrates the TV reception and relay methods at each node. In this architecture, WiFi routers, LTE, and 5G mmWave receivers are assumed to be mounted on top of the house to reduce fading and shadowing losses. Moreover, content can be relayed using either *all-or-nothing flows* or *fractional flows*. In all-or-nothing flows, a household receives all content from a single source/relay node; using fractional flows, a household receives content simultaneously from multiple sources/relays. TV traffic demand at household i is denoted by δ_i (in Mbps). The demand can also be expressed as $\psi_i * b$, where ψ_i is the number of channels being demanded at household i and b is the capacity required per channel in Mbps.

A. Relay Using WiFi

The WiFi relay network is modeled as an undirected graph $\mathcal{G} = (\mathcal{V}, \mathcal{E})$, where $\mathcal{V}$ is the set of households and $\mathcal{E}$ is the set of WiFi links between households. WiFi transmissions between neighboring households operate on orthogonal channels and are highly directional by making use of beam-forming techniques. Point-to-point connections among households avoid wasting airtime in collision avoidance. Furthermore, the households are bounded by a degree of connectivity represented by ρ, i.e., a household has a maximum of ρ point-to-point links with neighboring households. We assume all WiFi transmitters have the same transmit power P, and path losses (PL) between two households are the same along both directions ($\mathrm{PL}_{ij} = \mathrm{PL}_{ji}$, between household i and j) [27]. A WiFi link exists from household i to j if j lies within the communication range of i; specifically, if the received signal strength on j is greater than the receiver sensitivity [28],

$$P - \mathrm{PL}_{ij} \geq \xi; \quad \forall i, j \in \mathcal{V}, \tag{1}$$

where ξ is the WiFi receiver sensitivity, and it is assumed to be identical for all WiFi receivers. According to [29], the path loss on a WiFi link can be calculated as

$$\mathrm{PL}(d) = \begin{cases} L_{\mathrm{FS}}(d) + \mathrm{SF}; & \text{if } d < d_{\mathrm{BP}}, \\ L_{\mathrm{FS}}(d_{\mathrm{BP}}) + 35\log_{10}(\dfrac{d}{d_{\mathrm{BP}}}) + \mathrm{SF}; & \text{if } d \geq d_{\mathrm{BP}}, \end{cases} \tag{2}$$

where d is the distance between the transmitter and receiver, $L_{\mathrm{FS}}(d)$ is the free space path loss in dB, d_{BP} is the breakpoint distance and SF is shadow fading in dB. The free space path loss is defined as

$$L_{\mathrm{FS}} = 20\log_{10}(d) + 20\log_{10}(f) - 147.5, \tag{3}$$

where f is the carrier frequency. From the transmit power and path loss computed with equations (2),(3), the received signal strength at j can be calculated. We use the tables in [29] and [30] to map the received signal strength to the corresponding modulation and coding scheme and the achievable capacity of WiFi links.

B. Relay Using WiFi and LTE

LTE BSs can be additional injection points of live TV content, subject to the availability of LTE bandwidth at the BS. Let $\mathcal{L}$ indicate the set of LTE BSs having significant spare LTE resources, e.g., wireless spectrum. The network topology is augmented as $\mathcal{G}' = (\mathcal{V}', \mathcal{E}')$, with $\mathcal{V}' = (\mathcal{V} \cup \mathcal{L})$ and $\mathcal{E}'$ consisting of all WiFi and LTE links. LTE BSs can only be a source node. Thus, all LTE links in the topology are unidirectional from an LTE BS to households. An LTE BS uses a shared set of channels for transmission in its coverage area. Thus, resources must be shared between households receiving TV content from the same LTE BS. We use TDMA for resource sharing. Let $0 \le \lambda_{ij} \le 1$ be the timeshare of the link from LTE BS $i \in \mathcal{L}$ to household $j \in \mathcal{V}$, $\sum_j \lambda_{ij} \le 1$, $\forall i \in \mathcal{L}$. To characterize LTE links, the path loss from LTE BSs to households are obtained from 3GPP specifications [31]. Further, using the maximum allowed transmit power of LTE BSs and the path loss model, we evaluate the LTE capacity as [32],

$$C_{ij}^{\mathrm{LTE}} = \beta \mathcal{W} \log_2(1 + \gamma\, \mathrm{SNR}), \tag{4}$$

where β is the fraction of bandwidth ($\mathcal{W}$) used for data transmission while the rest is used for control signaling and γ is the fraction of the received signal to noise ratio that contributes to broadband speed.

C. Relay Using WiFi and 5G mmWave

We further explore the use of 5G mmWave at 73 GHz for live TV services using highly directional point-to-point connectivity. We consider replacing LTE radios with 5G radios at the existing LTE BSs. For the reliable provisioning of live TV services using mmWave, we need to evaluate the extreme atmospheric effects on mmWave propagation such as attenuation due to rain, snow, hail, fog, and oxygen and water vapor absorption [33]. Also, obstructions due to trees and buildings will be the major sources of penetration losses [34]. These different environmental conditions may result in different types of losses. However, the large available bandwidth in the mmWave bands can potentially provide higher data rate connectivity to households. At the same time, it is clear that we will have poor connectivity from existing BSs to some households due to obstructions. Thus, for the 5G millimeter wave scenario, we consider a two hop system architecture where a set of houses may receive content from 5G millimeter wave BSs depending upon their connectivity, and relay TV to other houses over WiFi. Additionally, some houses may still require satellite antennas if they cannot receive TV content from 5G BSs either directly or through a WiFi relay. To examine the feasibility of live TV services over 5G millimeter wave, we use path loss models that incorporate an empirical study of attenuation due to extreme environmental conditions, and the probability of LOS communication.

1) 5G mmWave Path Loss Models: For this work, we consider the close-in (CI) free-space reference distance path loss model for urban, suburban, and rural scenarios. The general expression for CI path loss model is given by [35]:

$$\mathrm{PL}^{\mathrm{CI}}(f_c, d_0)[\mathrm{dB}] = \mathrm{FSPL}(f_c, d_0)[\mathrm{dB}] + 10n\log_{10}\left(\frac{d}{d_0}\right) + \mathcal{X}_\sigma, \quad \text{where } d \ge d_0 \text{ and } d_0 = 1 \text{ m}. \tag{5}$$

here d is the distance between transmitter and receiver in meters, d_0 is the close-in free space reference distance in meters, n represents the path loss exponent (PLE), and f_c is the frequency in GHz. Further, shadow fading is represented by the zero-mean Gaussian random variable $\mathcal{X}_\sigma$ with standard deviation σ in dB. The first term in the equation (5) is the frequency dependent path loss up to the close-in reference distance $d_0 = 1$ m [35], and is equivalent to Friis' FSPL [35]:

$$\begin{aligned}\mathrm{FSPL}(f_c, d_0)[\mathrm{dB}] &= 20\log_{10}\left(\frac{4\pi f_c \times 10^9}{c}\right)\\ &= 32.4 + 20\log_{10}(f_c)\end{aligned} \tag{6}$$

PLE is dependent upon the surrounding conditions and can be considered between 2 and 5. For urban and suburban scenarios, we consider PLE $= 4.6$ and $\sigma = 8.54$ for both LOS and NLOS [36]. In the rural scenarios, the LOS and NLOS PLE is considered as 2.31 and 3.01, respectively [37]. Similarly, σ is considered as 5.9 dB and 8.2 dB for LOS and NLOS, respectively [37].

2) Atmospheric Effects on mmWave: As discussed previously, different atmospheric conditions can contribute to attenuation in the signal strength. However, the attenuation due to rainfall is the worst case atmospheric condition and can therefore be used in a conservative model [33]. Crane's theoretical prediction model, based on atmospheric temperature, rain rate, and rain structure, is summarized as [38],

$$A_R = \begin{cases} aR^b\left[\dfrac{e^{ubd}-1}{ub}\right]; & \text{if } 0 \le D \le d,\\ aR^b\left[\dfrac{e^{ubd}-1}{ub} - \dfrac{B^b e^{cbd}}{cb} + \dfrac{B^b e^{cbD}}{cb}\right]; & \text{if } d \le D \le 22.5\text{km}.\end{cases}$$

where, $u = \frac{ln(Be^{cd})}{d}$, $B = 2.3R^{-0.17}$, $c = 0.026 - 0.03ln(R)$, $d = 3.8 - 0.6ln(R)$ in km, A_R is the path loss attenuation due to rain in dB, R is the point rain rate in mm/hr, and D is the path length in km. Multipliers a and b are rain attenuation coefficients dependent on frequency and polarization. Values of parameters a and b are calculated at 73 GHz frequency as 1.099969083 and 0.711048, respectively [39].

3) LOS Probability: Finally, Table I presents the LOS probability model for urban, suburban, and rural scenarios [40].

For easy reference, the notation is presented in Table II.

TABLE I
LOS PROBABILITY

Scenarios	**LOS probability as a function of distance in [m]**
UMa	$P_{LOS} = min\left(\frac{18}{d}, 1\right)\left(1 - \left(e^{\frac{-d}{63}}\right)\right) + e^{\frac{-d}{63}}$
SMa	$P_{LOS} = 1,\ d \le 10$; else, $P_{LOS} = e^{\frac{-(d-10)}{200}}$
RMa	$P_{LOS} = 1,\ d \le 10$; else, $P_{LOS} = e^{\frac{-(d-10)}{1000}}$

TABLE II
NOTATION

Parameter	Description
$\mathcal{V}, \mathcal{L}, \mathcal{V}'$	Set of households, LTE BSs and both, respectively
$\mathcal{E}, \mathcal{E}'$	Set of WiFi links, set of WiFi and LTE links
$\mathcal{S}, \mathcal{R}, \mathcal{T}$	Set of Source, Relay and Terminal nodes, respectively
δ_i	Demand at household i
h	Maximum allowed hops in the topology
ρ	Maximum degree of connectivity at source and relay nodes
C_{ij}	Capacity of link from node i to j
s	Number of 802.11n parallel streams used

IV. Joint Optimization of Satellite Antenna Placement and Relay Routing

In this section, we develop optimization models to systematically evaluate the design trade-offs in WiLiTV. We consider the following routing complexity factors.

1) *Relay Hop Count:* Ideally, each connected island of households only needs one source, and TV content can be relayed to all households using an arbitrary number of hops. However, live TV services have stringent QoS requirements on delay, bandwidth, and reliability. It is well known that multi-hop wireless relays can lead to long delay, lower throughput, and poor reliability [41]. Thus, we limit relay routing to at most two hops.
2) *Splittable Flows:* As discussed in Section III, with fractional flows, one household can download content along multiple relay paths from multiple sources. This can potentially increase the wireless link utilization and coverage of each source, leading to higher cost savings. As with any multi-path routing, splittable flows have to deal with delay disparity on different paths, and data transmission reliability decreases as more links and nodes are employed. We will compare the efficiency of relay routing with and without splittable flows.
3) *LTE/5G mmWave Availability:* An LTE BS had wider coverage than a WiFi transmitter. But LTE bandwidth resources are limited and expensive. We will evaluate the coverage gain added by LTE BS to justify its bandwidth cost. On the other hand, 5G mmWave has poorer coverage area but large available bandwidth.
4) *Dynamic vs. Static Solution:* User TV demand naturally varies over time. To maximally reduce cost, one should design dynamic source provisioning and relay routing solutions to match the changing user demand. However, it is not practical to change satellite antenna locations on an hourly or daily basis, and reconfiguring relay routing may cause short-term service disruption. Static solutions are easier to implement. We will formally study the performance gap between dynamic and static solutions.

To systematically evaluate the impact of various source provisioning and relay routing strategies on cost saving, we formulate a series of joint provisioning-routing optimization problems to find the lowest costs under different routing constraints in this section. We consider two types of routing strategies, (i) static routing: routing is considered fixed to satisfy demand at different time periods in a day, (ii) reconfigurable routing: routing changes with demand over time. The first solution may require more satellite antennas. However, it is simpler to implement in practice. The second solution is practical and economical, since WiFi/LTE links and relay routing can be conveniently reconfigured using Software Defined Radio and/or Software Defined Networks. We will formulate an optimization problem for a reconfigurable routing strategy and further extend it to static routing.

A. All-or-Nothing Flow With Reconfigurable Routing

Our proposed WiLiTV architecture has a maximum relay hop count of two. Thus, there are three types of houses in the network: source nodes with satellite antennas, non-source nodes relaying video for other nodes (called relay nodes), and non-source nodes without any relayed traffic (called terminal nodes). Let $X_i \in \{0,1\}, \forall i \in \mathcal{V}$ be the binary variable indicating whether a node is equipped with a satellite antenna. We assumed satellite antenna positions will not be changed after the initial provisioning, thus X_i is not a function of time. Let $Y_i(t) \in \{0,1\}, i \in \mathcal{V}, \forall t \in \mathcal{T}$ be another binary variable indicating whether a node relays other nodes' traffic. A node can be dynamically selected to route other nodes' traffic, thus the binary variable $Y_i(t)$ is time-varying. For a source node we have $X_i = 1$ and $Y_i(t) = 0$, i.e., a source node does not relay other nodes' traffic. Similarly, for a relay node we have $X_i = 0$ and $Y_i(t) = 1$, and for a terminal node, we have $X_i = 0$ and $Y_i(t) = 0$. Similarly, let $u_{ij}(t) \in \{0,1\}, \forall \langle i,j\rangle \in \mathcal{E}, \forall t \in \mathcal{T}$ be the binary variable indicating if a link from node i to node j carries node j's TV demands. We introduce another binary variable $\Delta_i(t)$ such that if household i has TV traffic demand at time t, then $\Delta_i(t) = 1$, otherwise 0. Fig. 2 illustrates the three types of nodes in the two-hop relay, and how terminal nodes download video content from the source through a common relay node. Further, LTE resources are shared among all the houses that receive TV content from the same LTE BS. Let $0 \le \lambda_{ij}(t) \le 1$ be the time share of the link from LTE BS $i \in \mathcal{L}$ to house $j \in \mathcal{V}$, $\sum_j \lambda_{ij}(t) \le 1, \forall i \in \mathcal{L}, \forall t \in \mathcal{T}$. Using the previous variables, we can formulate a mixed-integer programming problem as follows:

$$\underset{\{X_i, Y_i(t), u_{ij}(t)\}}{\textbf{Minimize:}} \sum_{i \in \mathcal{V}'} X_i \tag{7}$$

$$\textbf{Subject to:} \sum_{j:\langle i,j\rangle \in \mathcal{E}'} u_{ij}(t) \le \rho(X_i + Y_i(t)), \quad \forall i \in \mathcal{V}', \quad \forall t \in \mathcal{T}; \tag{8}$$

$$\sum_{i:\langle i,j\rangle \in \mathcal{E}'} u_{ij}(t) = Y_j(t) + \Delta_j(t)(1 - X_j - Y_j(t)), \quad \forall j \in \mathcal{V}, \quad \forall t \in \mathcal{T}; \tag{9}$$

$$0 \le X_i + Y_i(t) \le 1, \quad \forall i \in \mathcal{V}', \ \forall t \in \mathcal{T}; \tag{10}$$

$$Y_j(t) \le 2 - Y_i(t) - u_{ij}(t), \quad \forall i, j \in \mathcal{V}', \quad \forall t \in \mathcal{T}; \tag{11}$$

$$u_{ij}(t)C_{ij} \ge \delta_j(t)u_{ij}(t) + \sum_{k:k \ne i,j} Y_k(t)\delta_k(t)u_{jk}(t), \quad \forall i, j, k \in \mathcal{V}, \quad \forall t \in \mathcal{T}; \tag{12}$$

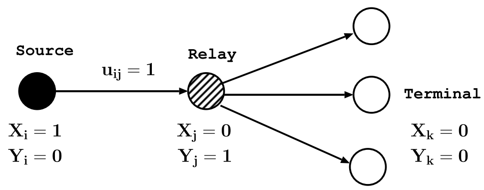

Fig. 2. Two-hop Relay Routing: node i is a source node ($X_i = 1$), node j is a relay ($Y_j = 1$), downloading traffic from i ($u_{ij} = 1$), relaying video to other terminal nodes ($X_k = Y_k = 0$).

$$\lambda_{ij}(t)C_{ij} \geq \delta_j(t)u_{ij}(t) + \sum_{k,k\neq i,j} Y_k(t)\delta_k(t)u_{jk}(t), \quad \forall i \in \mathcal{L}, \quad \forall j,k \in \mathcal{V}, \ \forall t \in \mathcal{T}. \quad (13)$$

The objective (7) is to minimize the number of satellite antennas. Constraint (8) bounds the maximum degree of connectivity at source and relay nodes (both have $X_i + Y_i(t) = 1$), and terminal nodes cannot have outgoing video traffic ($X_i + Y_i(t) = 0$). Constraint (9) says that node j needs to download video through exactly one incoming link if either j is a relay node ($Y_j(t) = 1$), or it is a terminal node ($X_j(t) = Y_j(t) = 0$) and has demand ($\Delta_j(t) = 1$). Constraint (10) states that a node in the distribution network can only assume one role: source, relay or terminal node at a given time instance. Constraint (11) ensures that a relay node does not receive traffic from another relay node at any given time instance. This is because if node j receives video from a relay node i, then $Y_i(t) = 1$ and $u_{ij}(t) = 1$. Then to make (11) hold, we must have $Y_j(t) = 0$, i.e, j cannot be a relay node anymore. On the other hand, if i is a source node, $Y_i(t) = 0$, even if $u_{ij}(t) = 1$, we can still have $Y_j(t) = 1$ (i.e., j can still relay video to other nodes). Constraint (12) guarantees each outgoing WiFi link from a source or relay has enough bandwidth to carry video traffic assigned to it. Similarly, constraint (13) ensure that each outgoing LTE link has enough bandwidth to carry video traffic assigned to them.

We can observe that the optimization problem in (7) – (13) is not a convex optimization problem due to constraints (12) and (13). Also, we want to evaluate the tradeoff of one-hop vs two-hop relay routing. Thus, we modify the optimization problem in (7) – (13) to make it convex and account for different relay routing scenarios.

1) One-Hop WiFi Relay: The network graph is given by $\mathcal{G}$, consisting only of houses. Furthermore, there will not be any relay node, i.e., $Y_i(t) = 0, \forall i \in \mathcal{V}, \forall t \in \mathcal{T}$. Thus, the optimization problem reduces to:

$$\underset{\{X_i, u_{ij}(t)\}}{\textbf{Minimize:}} \sum_{i\in\mathcal{V}} X_i$$

Subject to: (8), (9), and (12).

2) Two-Hop WiFi Relay: The network graph is given by $\mathcal{G}$, consisting of only houses. The WiFi network contains source nodes, relay nodes, and terminal nodes, i.e., a few of the nodes do not have $Y_i(t) = 0$ at a given time instance. Thus, constraint (12) is modified in the equation (14) to make it convex.

$$u_{ij}(t)C_{ij} \geq \delta_j(t)u_{ij}(t) + \sum_{k,k\neq i,j} \delta_k(t)u_{jk}(t) - \Theta(1-X_i-Y_i(t)), \quad \forall i,j,k\in\mathcal{V}, \ \forall t\in\mathcal{T}. \quad (14)$$

The first term on the right hand side of equation (14) is the video traffic from the source/relay node to its direct receiver. The second term is non-zero only if i is a source and j is a relay; it represents the traffic of all households downloading video from i through relay j. The last term is zero if i is a source or relay, and if i is a terminal node; Θ is a large number so that the inequality automatically holds. Thus, the optimization problem is modified as:

$$\underset{\{X_i, Y_i(t), u_{ij}(t)\}}{\textbf{Minimize:}} \sum_{i\in\mathcal{V}} X_i$$

Subject to: (8), (9), (10), (11) and (14).

3) One-Hop Relay Over LTE Overlay: The network graph is given by $\mathcal{G}'$, consisting of houses and LTE BSs. Further, there will not be any relay node in the network, i.e., $Y_i(t) = 0$, $\forall i \in \mathcal{V}, \forall t \in \mathcal{T}$. Thus, the optimization problem reduces to:

$$\underset{\{X_i, u_{ij}(t), \lambda_{ij}(t)\}}{\textbf{Minimize:}} \sum_{i\in\mathcal{V}'} X_i$$

Subject to: (8), (9), (12) and (13).

4) Two-Hop Relay Over LTE Overlay: The network graph is given by $\mathcal{G}'$, consisting of houses and LTE BSs. The network contains source nodes, relay nodes, and terminal nodes, i.e., a few of the nodes do not have $Y_i(t) = 0$ at a given time instance. Thus, constraint (13) is modified in the equation (15) below to make it convex.

$$\lambda_{ij}(t)C_{ij} \geq \delta_j(t)u_{ij}(t) + \sum_{k,k\neq i,j} \delta_k(t)u_{jk}(t) - \Theta(1-X_i-Y_i(t)), \quad \forall i\in\mathcal{L}, \ \forall j,k\in\mathcal{V}, \ \forall t\in\mathcal{T}. \quad (15)$$

Similar to (14), this constraint ensures that the link from BS i to household j carries the video demands of household j and all other households using j as a relay. The optimization problem reduces to:

$$\underset{\{X_i, Y_i(t), u_{ij}(t), \lambda_{ij}(t)\}}{\textbf{Minimize:}} \sum_{i\in\mathcal{V}'} X_i$$

Subject to: (8), (9), (10), (11), (14) and (15).

5) Two-Hop Relay Over 5G mmWave Overlay: The problem formulation for 5G mmWave overlay remains similar to LTE overlay. However, $\sum_j \lambda_{ij} \leq 1$, , $\forall i \in \mathcal{L}, \forall t \in \mathcal{T}'$, where $\mathcal{T}'$ is the set of houses that lies in the same angular space.

B. All-or-Nothing Flow With Static Routing

In the reconfigurable routing strategy, variables $Y_i(t)$, $u_{ij}(t)$, and $\lambda_{ij}(t)$ are functions of time to dynamically adapt to users demand. However, in a static strategy routing decisions are made once, such that routes can satisfy demand at any time. Thus, variables $Y_i(t)$, $u_{ij}(t)$, and $\lambda_{ij}(t)$ are no longer functions of time in the optimization problem. Furthermore,

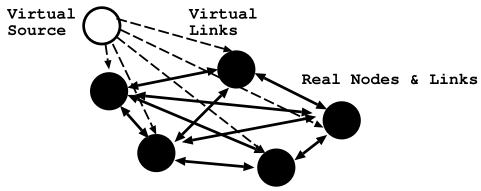

Fig. 3. Virtual network topology for splittable relay routing.

there should be one incoming link to each relay/terminal node irrespective of demand. Thus, the constraint (9) is modified in equation (16) as follows:

$$\sum_{i:\langle i,j\rangle\in\mathcal{E}'} u_{ij} = (1 - X_j), \quad \forall j \in \mathcal{V},\ \forall t \in \mathcal{T}. \tag{16}$$

The rest of the optimization constraints can be modified accordingly to account for static routing for each scenarios in the reconfigurable routing strategy.

C. Splittable Relay Routing With Average Hop-Count Limit

In the last two optimization formulations, we considered all-or-nothing flows and each household downloads all its video demands from only one source/relay node. To further improve the flexibility and efficiency of relay routing, a household can receive video from multiple sources and/or relays simultaneously through multiple relay paths. We develop a variation of the well-known multi-commodity flow problem to cover this case. As illustrated in Fig. 3, we first augment the distribution network with a virtual source node (indicated by s), that connects to all the nodes in the topology through virtual links with very high capacities. All video demands are served from the virtual source. If a household installs a satellite antenna, it is equivalent to saying that we activated its virtual link from the virtual source for direct video downloading. The objective of minimizing the number of satellite dishes is equivalent to minimizing the number of activated virtual links. We define a binary variable l_{si} indicating whether the virtual link from the virtual source s to node i is activated. We further define f_{ij} as the video traffic volume on link $\langle i, j\rangle$. The optimization with splittable relay routing can be formulated as the following mixed-integer programming problem.

$$\textbf{Minimize:}_{\{l_{si}\},\{f_{ij}(t)\}} \sum_{i\in\mathcal{V}'} l_{si} \tag{17}$$

$$\textbf{Subject to: } f_{si}(t) + \sum_{j:\langle j,i\rangle\in\mathcal{E}'} f_{ji}(t) = \delta_i(t) + \sum_{k:\langle i,k\rangle\in\mathcal{E}'} f_{ik}(t), \quad \forall i \in \mathcal{V}',\ \forall t \in \mathcal{T}; \tag{18}$$

$$\sum_{i\in\mathcal{V}'} f_{si}(t) = \sum_{i\in\mathcal{V}'} \delta_i(t), \quad \forall t \in \mathcal{T}; \tag{19}$$

$$f_{ij}(t) \le C_{ij}, \quad \forall\langle i, j\rangle \in \mathcal{E}',\ \forall t \in \mathcal{T}; \tag{20}$$

$$f_{si}(t) \le l_{si} C_{si}, \quad \forall i \in \mathcal{V}',\ \forall t \in \mathcal{T}; \tag{21}$$

$$\sum_{\langle i,j\rangle\in\mathcal{E}'} f_{ij}(t) \le h \sum_{i\in\mathcal{V}'} \delta_i(t), \quad \forall i \in \mathcal{V}',\ \forall t \in \mathcal{T}. \tag{22}$$

Constraint (18) is the *flow-conservation* law at node i, i.e., the total incoming traffic at node i (left-hand side) equals the sum of the demand of node i and the total outgoing traffic (right-hand side). Constraint (19) implies that all the video downloading traffic in the virtual graph originates from the virtual source. Constraint (20) guarantees traffic on each relay link is bounded by its capacity, and Constraint (21) makes sure that a virtual link can carry video traffic only if it is activated. Finally, the left-hand side of Constraint (22) is the total video traffic on all relay links, i.e., the sum of the traffic generated by all households on all links. For each household, the total traffic it generates on all links equals its total video demand multiplied by its average relay hop count. Constraint (22) effectively limits the average hop count to a constant h.

The optimization problem in the (17) – (22) considers a reconfigurable routing strategy where video traffic changes depending upon demand at different nodes. The static routing strategy can be formulated by a static flow on each link such that it can accommodate TV traffic demand at any given instance of time. Thus, flow on a link is not a function of time, instead each link in the graph will accommodate the maximum traffic flow to satisfy demand at each time period.

D. Static Peak Demand

The optimization problems discussed so far consider time-varying demand which results in the optimal provisioning of services. However, the required computational time and resources may be quite high. Thus, we further investigate the WiLiTV architecture using static peak demand where the distribution network handles each house's maximum demand over all time periods, that is to let $\delta_i^0 \triangleq \max_{t=1,\cdots,T} \delta_i(t), \forall t \in \mathcal{T}$. While considering static peak demand routing variables $Y_i(t)$, $u_{ij}(t)$, and $\lambda_{ij}(t)$ are no longer time-varying. Hence, we plug in the time-independent demands $\{\delta_i^0, i \in \mathcal{V}\}$ to the optimization problems in section IV-B to obtain static provisioning and relay routing solutions for each scenario. This over-provisioning might waste some resources (the required number of satellite antennas) while saving on computational time and computational resources.

E. WiFi Link Tolerance

We finally evaluate the maximum WiFi link degradation our proposed WiLiTV architecture can tolerate. For the assesment of WiFi link degradation, we assume splittable flows. Let us assume from the graph $\mathcal{G}$ that M nodes have been selected as source nodes indicated by $\mathcal{M}$, i.e., each node in the set $\mathcal{M}$ works as the source node only and is responsible for transmitting all the TV traffic in the topology. Let ψ be the WiFi link degradation coefficient. Our objective is to maximize ψ such that we can still provide live TV Services with required QoE. With this, we formulate a linear programming to evaluate maximum WiFi link degradation as:

$$\textbf{maximize:}_{\{\psi\},\{f_{ij}(t)\}} \ \psi \tag{23}$$

$$\textbf{Subject to: } \sum_{j:\langle j,i\rangle\in\mathcal{E}} f_{ji}(t) = \delta_i(t) + \sum_{k:\langle i,k\rangle\in\mathcal{E}} f_{ik}(t), \quad \forall i \in \mathcal{V},\ \forall t \in \mathcal{T}; \tag{24}$$

$$\sum_{i \in \mathcal{M}} \sum_{j \in \mathcal{V}} f_{ij}(t) = \sum_{j \in \mathcal{V}} \delta_j(t), \quad \forall t \in \mathcal{T}; \tag{25}$$

$$f_{ij}(t) \leq (1-\psi) C_{ij}, \quad \forall \langle i, j \rangle \in \mathcal{E}, \ \forall t \in \mathcal{T}; \tag{26}$$

$$\sum_{\langle i,j \rangle \in \mathcal{E}} f_{ij}(t) \leq h \sum_{i \in \mathcal{V}} \delta_i(t), \quad \forall i \in \mathcal{V}, \ \forall t \in \mathcal{T}. \tag{27}$$

Constraint (24) is the *flow-conservation* law at node i, i.e., the total incoming traffic at node i (left-hand side) equals the sum of the demand of node i and the total outgoing traffic (right-hand side). Constraint (25) implies that all the video downloading traffic originates from nodes in the set $\mathcal{M}$. Constraint (26) guarantees traffic on each relay link is bounded by its capacity after degradation. The explanation for constraint (27) is the same as constraint (22).

V. Approximation Algorithms

In Section IV, different scenarios are modeled either as binary programming or mixed-integer programming problems, which are both NP-hard problems. When the network size is small, one can use various optimization tools, such as CVX in MATLAB [42], to get the exact optimal provisioning and relay routing solutions. However, when the network size is large, the computation time might become prohibitive. In this section, we develop heuristic approximation algorithms to obtain close-to-optimal solutions for large networks.

The problem formulations in Sections IV-A1 and IV-A2 with static peak demand and static routing are similar to the classic set cover problem. Our objective is to determine the minimum number of nodes that can cover all the other nodes in a given directed graph $\mathcal{G}$ with limited link capacity. Let $\mathcal{A}$ denote the relay matrix, where $\mathcal{A}[i, j] = 1$ if and only if there is a wireless relay link from node i to j, and the capacity of link $\langle i, j \rangle$ is larger than δ_j, the total video demand of j. Let $\mathcal{B}(i) \triangleq \{j \in \mathcal{V} : \ \mathcal{A}[i, j] = 1\}$ be the set of nodes that can potentially download their TV demands from node i. Then call $\mathcal{B}(i)$ the bin of node i.

The one-hop and non-splittable relay problem formulated in Section IV-A1 can be approximately solved using the greedy heuristic algorithm defined in Algorithm 1 below. Let $\mathcal{S}$ be the set of chosen source nodes, and $\mathcal{T}$ the set of terminal nodes that receive their TV channels from some source node in $\mathcal{S}$. At each iteration, node i with the largest bin size is selected as a new source node. All nodes in node i's bin are added to the terminal node set $\mathcal{T}$. If i's bin has more than ρ nodes, then we randomly select ρ nodes to be covered by i. All the nodes in i's bin are added to the terminal node set. All links from i to its receivers are added to the relay topology. Our problem is different from the traditional set cover problem as each element of a bin has its own bin. Thus, after selecting a node as source, the nodes in its bin are not removed from the network, because they can still act as sources for other nodes in future iterations. As a result, when we select a new source, it might have been covered by some source node and added to the terminal set in previous iterations. We need to remove it from the terminal node set (line 10), and also remove its incoming video link from the relay topology (line 11). After we update the source and terminal node sets, all links going to source and terminal nodes no longer need to be considered, and thus are removed from the relay matrix. After the iterations, nodes that are not marked as either source or terminal node are isolated nodes that need satellite antennas. Finally, the relay topology and source set are returned.

Algorithm 1 Greedy Algorithm for One-Hop Non-Splittable Relay

Input: Relay matrix ($\mathcal{A}$)
Output: Satellite antennas positioning and one-hop relay topology

1: **Initialization:** $\mathcal{S} \leftarrow \phi$, $\mathcal{T} \leftarrow \phi$, $\mathcal{A}_{tmp} \leftarrow \mathcal{A}$, $\mathcal{A}_{opt} \leftarrow \phi$
2: **while** $\mathcal{A}_{tmp}$ is not empty **do**
3: *Calculate* the bin of each node based on $\mathcal{A}_{tmp}$, and find node i with the largest bin.
4: $\mathcal{S} = \mathcal{S} \cup \{i\}$
5: **if** $|\mathcal{B}(i)| \leq \rho$ **then**
6: $\mathcal{R}(i) = \mathcal{B}(i)$
7: **else**
8: randomly select ρ nodes in $\mathcal{B}(i)$ to $\mathcal{R}(i)$.
9: **end if**
10: $\mathcal{T} = \mathcal{T} \cup \mathcal{R}(i) - \{i\}$
11: $\mathcal{A}_{opt} = \mathcal{A}_{opt} \cup \{\langle i, k \rangle, \forall k \in \mathcal{R}(i)\} - \{\langle k, i \rangle, \forall k \in \mathcal{V}\}$
12: $\mathcal{A}_{tmp} = \mathcal{A} - \{\mathcal{A}(m, n) : m \in \mathcal{V}, n \in \mathcal{S} \cup \mathcal{T}\}$
13: **end while**
14: **return** relay topology $\mathcal{A}_{opt}$ and source set $\mathcal{S}_{opt} = (\mathcal{V} - \mathcal{S} - \mathcal{T}) \cup \mathcal{S}$

Algorithm 1 can be extended to cover the two-hop non-splittable relay case. Similar to the one-hop case, we develop a greedy iterative algorithm. At each iteration, we add node i with the largest number of one-hop children as a new source. The links from node i to their children $\mathcal{R}(i)$ are added to the relay topology. Different from the one-hop case, some nodes in $\mathcal{R}(i)$ might further act as relays and forward video to two-hop children of i. Let $\mathcal{D}(i, \mathcal{R}(i))$ be the set of nodes connecting to i through $\mathcal{R}(i)$, i.e.,

$$\mathcal{D}(i, \mathcal{R}(i)) \triangleq \{k \in \mathcal{V} : \ \exists j \in \mathcal{R}(i) \text{ such that } C_{jk} \geq \delta_k\}.$$

Note that a node $k \in \mathcal{D}(i, \mathcal{R}(i))$ might connect to i through multiple relay nodes in $\mathcal{R}(i)$), and can be added as a two-hop child of i through any one of them in the relay topology. To build the two-hop relay tree rooted at i, we develop another greedy iterative algorithm. The outline of the algorithm is:

1) We first build the one-hop relay tree from i to $\mathcal{R}(i)$, and update the spare capacity on link $\langle i, j \rangle$, $j \in \mathcal{R}(i)$ as $\tilde{C}_{ij} = C_{ij} - \delta_j$.
2) We select the node, say j_0, with the highest spare capacity from node i to grow the second hop relay.
3) Among all children of j_0, we first select a node k that is connected to i only through j_0; if no such node exists, we randomly select a child k of j_0. If $\tilde{C}_{ij_0} \geq \delta_k$, we add k as a two-hop child of i through j_0 in the relay topology, and update the spare capacity $\tilde{C}_{ij_0} = \tilde{C}_{ij_0} - \delta_k$. If no child of j_0 can be added to the relay topology, we set $\tilde{C}_{ij_0} = 0$.
4) Go back to Step 2, *unless* either the spare capacity of all first-hop links originated from node i become zero, or all nodes in $\mathcal{D}(i, \mathcal{R}(i))$ are added to the relay topology.

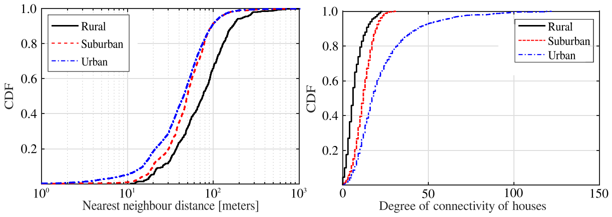

(a) (b)

Fig. 4. (a) CDF plot of the distance of the nearest neighbor to houses, (b) CDF plot of degree of connectivity to houses.

After we build the two-hop relay tree rooted as node i, we move on to find the next source with the highest degree until all the nodes are covered.

VI. Performance Evaluation

We evaluate the proposed WiLiTV architecture using real home locations and user demand data from a major USA-based ISP. We focus on data from three representative residential areas: urban (San Diego, California), suburban (Valencia, California), and rural (Canyon Country, California). The corresponding topologies consist of $22,606$, $1,914$, and 805 houses, respectively. The details of the three considered topologies are presented in the Fig. 4. Fig. 4(a) plots the Cumulative Distribution Function (CDF) of the distance of the nearest neighboring house to each house. We can observe from the figure that in the rural area around 60% of the houses have their nearest neighboring house located within 100 meters. By contrast, for suburban and urban areas, approximately 90% of the houses have the nearest neighboring house within 100 meters. Note that by using an Effective Isotropic Radiated Power (EIRP) of 36 dBm and 20° phase-array antennas, we can achieve a range of 230 meters for WiFi in the 5 GHz band using an 802.11n radio [43]. Fig. 4(b) presents the CDF plot of the degree of connectivity between houses in rural, suburban, and urban areas according to the IEEE 802.11n path loss model. From the figure, we can observe a high degree of connectivity between houses for the urban scenario. In the rural scenario, around 5% of houses are standalone houses, given their sparse connectivity.

Using the optimization formulations in Section IV, we find the optimal source provisioning and relay topologies under different relay routing constraints. We first conduct an evaluation with static video demands for all-or-nothing flows, where each house's demand is its peak over all time periods and each house receives TV traffic through only one source/relay node. We then conduct an evaluation with time varying demands and splittable flows. We further explore the use of *parallel streams* supported in IEEE 802.11n. Using parallel streams, data can be split and transmitted via multiple independent data streams. Thus, with spatial separation of signals by antennas using beam-forming and Multiple Input, Multiple Output (MIMO) antenna techniques, up to four parallel streams can be supported in IEEE 802.11n.

Fig. 5 shows the average TV traffic demand pattern over a day in the urban scenario. In the rural and suburban scenarios,

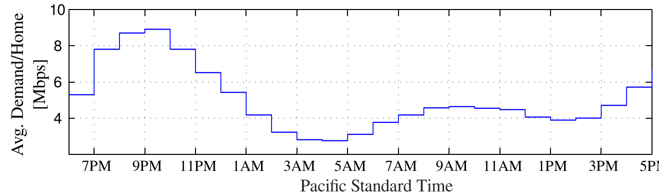

Fig. 5. Average TV traffic demand in San Diego.

we obtain a similar pattern for demand. From the real demand data of TV channels for each house at each hour of a day, obtained from a service provider, we computed the capacity required for HDTV transmissions. The TV traffic demand is assumed constant for the entire duration of an hour.

The carrier frequency for 802.11n radios is 5 GHz and the channel bandwidth used is 20 MHz. For simplicity of the topology, we assumed that a house can connect to a maximum of 5 neighboring houses. We assumed that 10%, 20%, and 30% of total LTE bandwidth is available for WiLiTV service in the urban, suburban and rural scenarios, respectively.

To evaluate the 5G mmWave saving, we consider the same system setup as in [37]. 5G BSs are equipped with a large number of horn antennas, each with a 7° azimuth and half-power beamwidth (HPBW) and an antenna gain of 27 dBi. An identical antenna setup with 27 dBi of gain and 7° azimuth and elevation HPBW is assumed at the receiver to capture the RF signal. Further, we kept transmit EIRP of 5G radios the same as LTE radios, i.e., 46 dBm transmit EIRP. We assume the available bandwidth at each 5G BS as 800 MHz at the 73 GHz carrier frequency. To get a worst case scenario, we assume heavy rain with a rain rate of 50 mm/hr.

A. Static Peak Demand

Fig. 6 plots the percentage saving in the required satellite antennas for live TV content distribution in different scenarios for different topologies. With one IEEE 802.11n stream and a single hop over the WiFi network, 65%, 77%, and 80% of satellite antennas can be saved for the rural, suburban, and urban scenarios. With four WiFi streams over two hops, savings in the required satellite antennas increases to 82%, 85% and 88% for the rural, suburban, and urban scenarios. *This suggests that additional WiFi link capacities resulting from more streams directly translate into cost savings in satellite antennas, especially with two-hop relays.* From Fig. 6(c), we can observe some saving in the required satellite antennas in the rural scenario due to a large amount of available LTE bandwidth. However, we do not observe any gain in saving in the required satellite antennas for suburban and urban scenarios due to the congested LTE bandwidth assumption. A similar observation can be seen for 5G mmWave in the rural, suburban, and urban environment. Due to high 5G mmWave capacity and relatively few obstructions in a rural scenario, we observe saving in the required satellite antennas as high as 85.2%. We expect that given our conservative assumptions for rural mmWave, as this technology matures and improves, *mmWave technology with WiFi may be a promising option for rural broadband*. However, in the suburban and urban

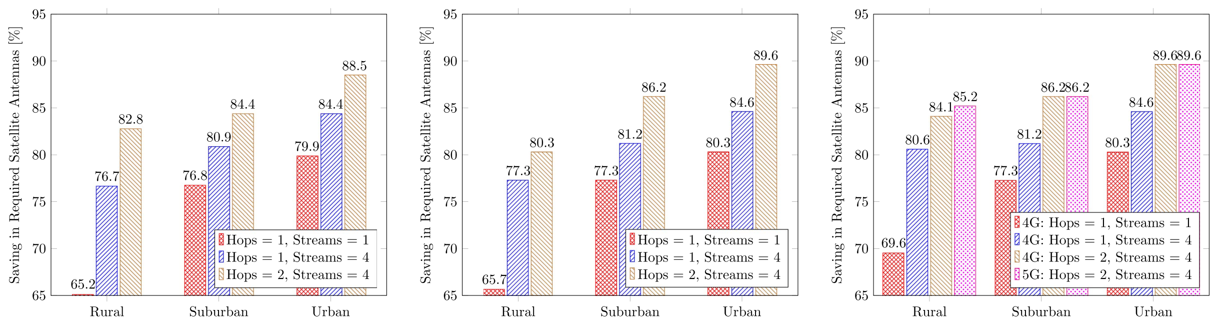

(a) WiFi: heuristic algorithm (b) WiFi: branch-and-bound (c) LTE/5G overlay: branch-and-bound

Fig. 6. Static peak demand and all-or-nothing flow: saving in the required number of satellite antennas for live TV services.

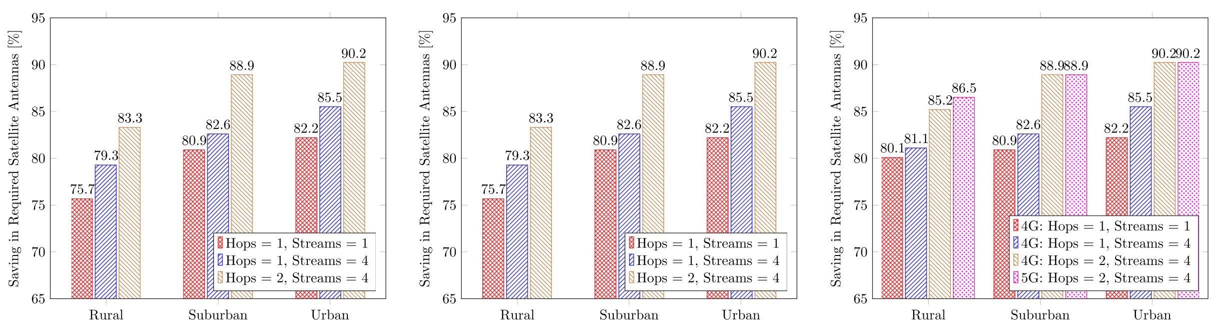

(a) WiFi: static routing (b) WiFi: reconfigurable routing (c) LTE/5G overlay: Static routing

Fig. 7. Time-varying demand and all-or-nothing flow: saving in the required number of satellite antennas for live TV services.

scenarios, we do not observe a further saving in the required satellite antennas due to higher path loss at 73 GHz in the urban and suburban environment. This supports the fact that in urban and suburban scenarios, densification of 5G mmWave BSs is required to deliver enough capacity.

Fig. 6(a) and 6(b) compares the results of branch-and-bound with our proposed heuristic algorithms. Using branch-and-bound over a single hop, we obtain the optimal solution for the rural, suburban, and urban topologies. Our proposed heuristic algorithm can always gets close to the optimal solutions for all three scenarios in $O(VE)$ runtime, while other optimization algorithms such as branch-and-bound take exponential runtime.

B. Time-Varing Demand

Fig. 7 plots the percentage saving in the number of required satellite antennas for time-varying demand for both static and reconfigurable routing strategies. For time-varying demand, we presented a multi-hour provisioning formulation in Sections IV-A (reconfigurable routing) and IV-B (static routing). Fig. 7 compares the required satellite antennas to satisfy TV traffic demands at all time instants to results obtained for fixed peak TV demands in Fig. 6, all with non-splittable relays. *This suggests that formulations considering time-varying demand, instead of per-user peak demands, can lead to a higher cost saving*. The additional saving in the required satellite antennas is obtained due to resource multiplexing in the case of multi-hour provisioning which exploits the varying demand coming from different homes at a given hour. We achieve a higher saving in the required satellite antennas at the cost of additional computation time complexity. However, routes are computed only at setup or in a failure scenario. Further, Fig. 7(a) and Fig. 7(b) compare the saving in required satellite antennas for static and reconfigurable routing strategies over a WiFi network. The same results were obtained for both routing strategies. *This suggests that the ability to reconfigure routing does not lead to significant savings for all-or-nothing flows*. Thus, we only present savings in the number of required satellite antennas for the LTE/5G mmWave overlay in Fig. 7(c) for the static routing strategy. The explanation for the additional savings in required satellite antennas for LTE/5G mmWave overlay and time-varying demand is the same as in the case of static peak demand.

C. Splittable Flow

Finally, an optimal distribution topology is obtained for splittable flows for static and reconfigurable routing, as discussed in Sections IV-C. We obtain results for splittable flows using an average hop count of two, and one to four parallel streams, as shown in Fig. 8. As traffic can be routed from multiple sources and over different routes, we thus obtain further savings (however, not significant) in the required satellite antennas. While there is no significant saving in the required satellite antennas while incurring higher computational complexity, splittable relaying can achieve higher reliability where network coding techniques can exploit the diversity of different

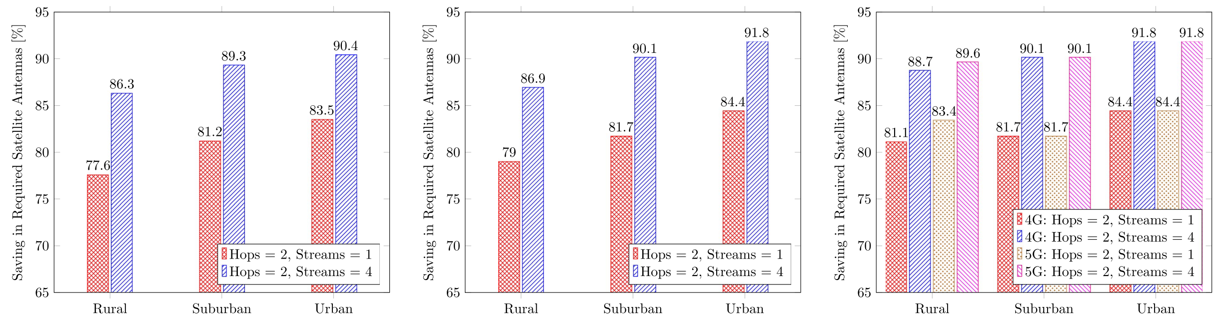

(a) WiFi: static Routing (b) WiFi: reconfigurable routing (c) LTE/5G overlay: reconfigurable routing

Fig. 8. Splittable Flow: saving in the required number of satellite antennas for live TV services.

TABLE III
SAVINGS FOR DIFFERENT TV FORMATS [%]

Scenario	**SDTV**	**HDTV**	**4K**
Rural	86.9	86.9	79.2
Suburban	90.1	90.1	84.5
Urban	91.8	91.8	88.8

TABLE IV
MAXIMUM WIFI DEGRADATION TOLERANCE [%]

Scenario	**Hops = 2, Streams = 1**	**Hops = 2, Streams = 4**
Rural	7.72	17.14
Suburban	25.49	27.25
Urban	27.25	34.55

paths to add extra reliability. Network coding techniques for WiLiTV architectures can be studied in future work.

D. Robustness to Different Data Rates

Previous results considered HDTV at every household. Next, we evaluate WiLiTV for three types of TV services, (i) SDTV (2 Mbps), (ii) HDTV (9 Mbps), and (iii) 4K TV content (15.6 Mbps) using splittable flow and reconfigurable relay routing. Table III presents the savings in the required satellite antennas for different TV formats for two hops and four streams. We can observe from the table that we require a few more satellite antennas for the 4K TV. However, the increment in the required satellite antennas is not significant. *The analysis shows that our proposed WiLiTV architecture is robust even with an increase in required data rates.*

E. Effect of WiFi Channel Degradation

Next, we presents the effect of WiFi channel degradation on WiLiTV. Table IV presents the maximum WiFi channel degradation WiLiTV can tolerate in different topologies for reconfigurable routing. In the rural scenario, maximum allowed degradation in WiFi channel is low for both one and four streams. This happens due to relatively poor and sparse connectivity. However, in suburban and urban scenarios a higher degradation in WiFi channel can be tolerated.

TABLE V
COST OF DIFFERENT SCENARIOS OF WILITV W.R.T. TRADITIONAL SATELLITE TV ARCHITECTURE [IN MILLION US$]
(SPD: STATIC PEAK DEMAND, LTEO: LTE OVERLAY, TVD: TIME-VARYING DEMAND, SF: SPLITTABLE FLOW, NRR: NON-RECONFIGURABLE ROUTING, AND RR: RECONFIGURABLE ROUTING)

Scenario	**Rural**	**Suburban**	**Urban**
Traditional Satellite TV Architecture	0.73	1.75	20.70
WiFi-SPD (h=1, s=1)	0.45	0.92	9.55
WiFi-SPD (h=1, s=4)	0.36	0.86	8.62
WiFi-SPD (h=2, s=4)	0.32	0.77	7.77
LTEO-SPD (h=1, s=1)	0.43	0.92	9.55
LTEO-SPD (h=1, s=4)	0.34	0.86	8.62
LTEO-SPD (h=2, s=4)	0.31	0.77	7.77
WiFi-TVD (h=1, s=1)	0.37	0.86	9.07
WiFi-TVD (h=1, s=4)	0.35	0.83	8.39
WiFi-TVD (h=2, s=4)	0.31	0.72	7.42
LTEO-TVD (h=1, s=1)	0.35	0.86	9.07
LTEO-TVD (h=1, s=4)	0.33	0.83	8.39
LTEO-TVD (h=2, s=4)	0.30	0.72	7.42
WiFi-SF-NRR (h=2, s=1)	0.36	0.86	8.80
WiFi-SF-NRR (h=2, s=4)	0.29	0.71	7.37
WiFi-SF-RR (h=2, s=1)	0.35	0.85	8.62
WiFi-SF-RR (h=2, s=4)	0.29	0.70	7.08
LTEO-SF-RR (h=2, s=1)	0.34	0.85	8.62
LTEO-SF-RR (h=2, s=4)	0.28	0.70	7.08

This demonstrates that a modest over-provisioning of satellite antennas is sufficient to tolerate WiFi channel degradation.

VII. LIVE TV PROVISIONING COST COMPARISON

Finally, we compare our proposed WiLiTV architecture cost in different scenarios with the traditional satellite TV architecture. In all of the three topologies considered in this work, satellite installation costs around $915.57 per house [13]. Outdoor WiFi router installation costs around $125-$300 per house [44]. Similarly an LTE modem and antenna installation costs around $250 per house [45]. Table V indicates the cost associated with different scenarios of WiLiTV architecture with the traditional satellite TV architecture. While Table V may not be a complete measure of cost, we believe it serves the purpose of driving the design process of WiLiTV architecture towards minimizing the cost of live TV content distribution architectures. Using all-or-nothing flows and a WiFi network the cost of provisioning live TV services can be reduced by 56.76%, 58.78%, and 64.16% in rural, suburban, and urban scenarios, respectively. Similarly, using all-or-nothing flows and LTE overlay the cost of provisioning live TV services can be reduced by 58.36%, 58.78%, and 64.16% in rural, suburban, and urban scenarios, respectively. Using splittable flows and a WiFi network, the cost of provisioning live TV services can be reduced by 60.36%, 59.98%, and 65.76% in rural, suburban, and urban scenarios, respectively. Similarly, using splittable flows and an LTE overlay the cost of provisioning live TV services can be reduced by 61.66%, 59.98%, and 65.76% in rural, suburban, and urban scenarios, respectively. *To summarize, this study shows us that approximately 60% cost savings can be achieved for rural, suburban, and urban topologies using the WiLiTV architecture.*

VIII. Conclusion

In this paper, we propose an all-wireless solution to deliver live TV services. Some service providers now have the option of leveraging a combination of different wireless access technologies (satellite, WiFi, and 4G LTE/5G mmWave) to distribute live TV content. We capitalize on this opportunity to create a distribution infrastructure that is optimized to serve large residential neighborhoods with the minimal number of TV content injection points. We developed multi-commodity optimization flow problems to model various scenarios. Our results cover three different representative residential neighborhoods (rural, suburban, and urban) with time-varying traffic demands. Using real data from a national TV service provider, we show that our proposed architecture can save provisioning costs by 60%. Our results shows that backhauling from TV injection points (using existing LTE BSs) to households using 5G mmWave and connecting homes in coverage holes using a local WiFi network can save considerably on the cost of multimedia distribution, particularly in rural scenarios. Our investigation shows that there is an optimum strategy for placing the satellite dish antennas, combined with an appropriate selection of WiFi relay routes, to meet the TV content demand of subscribers. Further, we show that our proposed WiLiTV architecture is capable of providing high-quality TV services, even with a certain percentage of link degradation, and is robust in its support of different TV formats.

References

[1] K. Brunnström *et al.*, "Future media distribution: An innovation agenda for digital media distribution," Swedish ICT, Stockholm, Sweden, Tech. Rep., Feb. 2015. [Online]. Available: https://www.swedishict.se/sites/defauit/fies/pub/swedishict.se/rapport_sia_3_2_orig_web.pdf

[2] J. C. Ulin, *The Business of Media Distribution: Monetizing Film, TV, and Video Content in an Online World*. Boca Raton, FL, USA: CRC Press, 2013.

[3] X. Hei, C. Liang, J. Liang, Y. Liu, and K. W. Ross, "A measurement study of a large-scale P2P IPTV system," *IEEE Trans. Multimedia*, vol. 9, no. 8, pp. 1672–1687, Dec. 2007.

[4] K. Kerpez, D. Waring, G. Lapiotis, J. B. Lyles, and R. Vaidyanathan, "IPTV service assurance," *IEEE Commun. Mag.*, vol. 44, no. 9, pp. 166–172, Sep. 2006.

[5] FCC. *Broadband Speed Test (Mbps)*. Accessed: Jun. 30, 2014. [Online]. Available: https://www.broadbandmap.gov/summarize/nationwide

[6] R. N. Clarke, "Costs of neutral/unmanaged IP networks," *Rev. Netw. Econ.*, vol. 8, no. 1, pp. 61–89, Mar. 2009.

[7] J. Baliga, K. Hinton, and R. S. Tucker, "Energy consumption of the Internet," in *Proc. IEEE COIN-ACOFT*, Jun. 2007, pp. 1–3.

[8] U.S. Department of Transportation. (Nov. 2012). *Unit Cost Entries for Fiber Optic Cable Installation*. [Online]. Available: http://www.itskrs.its.dot.gov/

[9] DigitalAir. *Outdoor Wireless*. Accessed: Jun. 9, 2016. [Online]. Available: http://www.digitalairwireless.com/outdoor-wireless-networks.html

[10] LigoWave. *Infinity 802.11ac Series Access Points*. Accessed: Apr. 12, 2017. [Online]. Available: https://www.ligowave.com/products/nft-series

[11] B. G. Evans, "The role of satellites in 5G," in *Proc. ASMS/SPSC*, Sep. 2014, pp. 197–202.

[12] W. Feng, Y. Li, D. Jin, L. Su, and S. Chen, "Millimetre-wave backhaul for 5G networks: Challenges and solutions," *Sensors*, vol. 16, no. 6, p. 892, 2016.

[13] homewyse. *Cost to Install a Satellite Dish*. Accessed: Jul. 28, 2016. [Online]. Available: http://www.homewyse.com/services/cost_to_install_satellite_dish.html

[14] M. Wittig, "Satellite onboard processing for multimedia applications," *IEEE Commun. Mag.*, vol. 38, no. 6, pp. 134–140, Jun. 2000.

[15] ITU-R Regulation. (2016). *Radio Reguiations: Radio Sation and Systems—Article 1.39*. [Online]. Available: http://search.itu.int/history/HistoryDigitaiCoiiectionDocLibrary/1.43.48.en.101.pdf

[16] G. Gardikis and A. Kourtis, "Using DVB-S2 adaptive coding and modulation for the provision of satellite triple play services," *IEEE Commun. Mag.*, vol. 46, no. 12, pp. 128–135, Dec. 2008.

[17] G. Boccolini *et al.*, "UNIC: A novel bi-directional satellite-based platform to provide TV-centric triple play services," in *Proc. Mobile Wireless Commun. Summit*, Jul. 2007, pp. 1–5.

[18] M.-S. Shin, J. Ryu, D. Oh, and Y.-G. Kim, "The feasibility study on the 4K-UHD satellite broadcasting service in Ka-band," in *Proc. ICCE*, Jan. 2013, pp. 482–483.

[19] S. Morosi, E. Del Re, S. Jayousi, and R. Suffritti, "Hybrid satellite/terrestrial cooperative relaying strategies for DVB-SH based communication systems," in *Proc. IEEE EW*, May 2009, pp. 240–244.

[20] A. Iqbal and K. M. Ahmed, "Outage probability analysis of multi-hop cooperative satellite-terrestrial network," in *Proc. IEEE ECTI-CON*, May 2011, pp. 256–259.

[21] G. Cocco, N. Alagha, and C. Ibars, "Cooperative coverage extension in vehicular land mobile satellite networks," *IEEE Trans. Veh. Technol.*, vol. 65, no. 8, pp. 5995–6009, Aug. 2016.

[22] Y. Liu, Z. Liu, X. Wu, J. Wang, and C. C.-Y. Yang, "IPTV system design: An ISP's perspective," in *Proc. IEEE CyberC*, Oct. 2011, pp. 234–240.

[23] P. Paul and S. V. Raghavan, "Survey of multicast routing algorithms and protocols," in *Proc. ACM ICCC*, Aug. 2002, p. 902.

[24] A. Abdollahpouri, B. E. Wolfinger, and J. Lai, "Unicast versus multicast for live TV delivery in networks with tree topology," in *Proc. ACM WWIC*, Jun. 2010, pp. 1–14.

[25] A. Ksentini, M. Naimi, and A. Gueroui, "Toward an improvement of H.264 video transmission over IEEE 802.11e through a cross-layer architecture," *IEEE Commun. Mag.*, vol. 44, no. 1, pp. 107–114, Jan. 2006.

[26] R. Kumar, R. S. Margolies, R. Jana, Y. Liu, and S. Panwar, "WiLiTV: A low-cost wireless framework for live TV services," in *Proc. INFOCOM WKSHPS CNTCV*, May 2017, pp. 706–711.

[27] K. Pahlavan and A. H. Levesque, *Wireless Information Networks*. Hoboken, NJ, USA: Wiley, 1995.

[28] X. Li, "Collaborative localization with received-signal strength in wireless sensor networks," *IEEE Trans. Veh. Technol.*, vol. 56, no. 6, pp. 3807–3817, Nov. 2007.

[29] E. Perahia and R. Stacey, *Next Generation Wireless LANs: 802.11n and 802.11ac*. Cambridge, U.K.: Cambridge Univ. Press, 2013.

[30] *IEEE Standard for Information Technology—Telecommunications and Information Exchange Between Systems Local and Metropolitan Area Networks—Specific Requirements Part 11: Wireless LAN Medium Access Control (MAC) and Physical Layer (PHY) Specifications*, IEEE Standard 802.11-2012, 2012.

[31] *Technical Specification Group Radio Access Network; Evolved Universal Terrestrial Radio Access (E-UTRA); Base Station (BS) Radio Transmission and Reception (Release 10)*, document 3GPP TS 36.104 V10.2.0 (2011-04), 3GPP, 2011.

[32] P. Mogensen *et al.*, "LTE capacity compared to the Shannon bound," in *Proc. IEEE VTC*, Apr. 2007, pp. 1234–1238.
[33] S. J. Dudzinsky, "Atmospheric effects on terrestrial millimeter-wave communications," in *Proc. 4th Eur. Microw. Conf.*, 1974, pp. 197–201.
[34] T. S. Rappaport and S. Deng, "73 GHz wideband millimeter-wave foliage and ground reflection measurements and models," in *Proc. IEEE ICC Workshop*, Jun. 2015, pp. 1238–1243.
[35] T. Rappaport, *Wireless Communications: Principles and Practice*, 2nd ed. Englewood Cliffs, NJ, USA: Prentice-Hall, 2001.
[36] H. C. Nguyen, G. R. MacCartney, T. Thomas, T. S. Rappaport, B. Vejlgaard, and P. Mogensen, "Evaluation of empirical ray-tracing model for an urban outdoor scenario at 73 GHz E-band," in *Proc. VTC*, Sep. 2014, pp. 1–6.
[37] G. R. MacCartney and T. S. Rappaport, "Rural macrocell path loss models for millimeter wave wireless communications," *IEEE J. Sel. Areas Commun.*, vol. 35, no. 7, pp. 1663–1677, Jul. 2017.
[38] R. K. Crane, *Electromagnetic Wave Propagation Through Rain*. New York, NY, USA: Wiley, 1996.
[39] S. Shrestha and D. Y. Choi, "Rain attenuation statistics over millimeter wave bands in South Korea," *J. Atmospheric Solar-Terrestrial Phys.*, vols. 152–153, pp. 1–10, Jan. 2017.
[40] *Guidelines for Evaluation of Radio Interface Technologies for IMT-Advanced*, document ITU-R M.2135-1 Std., Dec. 2009.
[41] L. Gouveia, "Multicommodity flow models for spanning trees with hop constraints," *Eur. J. Oper. Res.*, vol. 95, no. 1, pp. 178–190, 1996.
[42] M. Grant and S. Boyd. (Mar. 2014). *CVX: MATLAB Software for Disciplined Convex Programming, Version 2.1*. [Online]. Available: http://cvxr.com/cvx
[43] U. Paul, R. Crepaldi, J. Lee, S.-J. Lee, and R. Etkin, "Characterizing WiFi link performance in open outdoor networks," in *Proc. IEEE SECON*, Jun. 2011, pp. 251–259.
[44] A. Gunn. *How Much Does it Cost to Build a Commotion Network?*. [Online]. Available: https://commotionwireless.net/blog/2014/04/14/how-much-does-it-cost/
[45] Amazon. *Netgear 4G LTE Modem*. Accessed: Apr. 10, 2017. [Online]. Available: https://www.amazon.com/NETGEARLLB1120L100NASLLTELModemLConnection/dp/B01MQRHQW4/ref=sr_1_2?Qs=eiectronics&ie=UTF8&qid=1519425475&sr=1L2&keywords=Netgear%2BLTE%2BModem&th=1

Rajeev Kumar received the B.Tech. and M.Tech. degrees in electrical engineering from IIT Madras, Chennai, India, in 2013. He is currently pursuing the Ph.D. degree in electrical engineering with the Tandon School of Engineering, New York University, Brooklyn, NY, USA. His research interests include 5G core network design, latency issues related to 5G networks, and network design for the delivery of multimedia services.

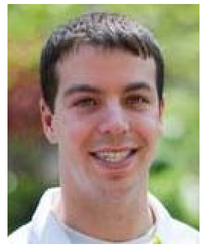

Robert Margolies (S'13–M'17) received the B.S. degree (*summa cum laude*) from the Rensselaer Polytechnic Institute in 2010 and the M.S. and Ph.D. degrees from Columbia University in 2011 and 2015, respectively, all in electrical engineering. He was a Senior Inventive Scientist with AT&T Research. He is currently a Senior Software Engineer with Google, NY, USA. His research interests are in cross-layer PHY and MAC layer design for ultra-low-power networks, networks of energy harvesting nodes, and opportunistic cellular scheduling.

Rittwik Jana received the Ph.D. degree in telecommunications engineering from the Australian National University, Canberra, Australia, in 2000. He is currently the Director of inventive science with AT&T Labs Research. His research interests span intelligent service composition of VNFs using TOSCA, model-driven control loop and automation in ONAP, networked video streaming, and wireless communications and systems.

Yong Liu (F'17) received the Ph.D. degree from the Electrical and Computer Engineering Department, University of Massachusetts, Amherst, in 2002. He is currently an Associate Professor with the Electrical and Computer Engineering Department, NYU Tandon School of Engineering. His general research interests lie in modeling, design, and analysis of communication networks. His current research directions include multimedia networking, network measurement and analytics, software-defined networks, online social networks, and recommender systems. He is a member of the ACM. He has served as an Associate Editor for the IEEE/ACM TRANSACTIONS ON NETWORKING, and the *Computer Networks* (Elsevier) Journal.

Shivendra S. Panwar (S'82–M'85–SM'00–F'11) received the Ph.D. degree in electrical and computer engineering from the University of Massachusetts, Amherst, in 1986. He is currently a Professor with the Electrical and Computer Engineering Department, NYU Tandon School of Engineering. He is also the Director of the New York State Center for Advanced Technology in Telecommunications, the Faculty Director and a Co-Founder of the New York City Media Laboratory, and a member of the NYU Wireless. His research interests include the performance analysis and design of networks. Current work includes cooperative wireless networks, switch performance, and multimedia transport over networks. He has co-authored a textbook *TCP/IP Essentials: A Lab Based Approach* (Cambridge University Press). He was a recipient of the IEEE Communication Society's Leonard Abraham Prize for 2004. He has served as the Secretary of the Technical Affairs Council of the IEEE Communications Society.